Proceedings of the
Annual Stability Conference
Structural Stability Research Council
Grapevine, Texas, April 18-21, 2012

Moment-shear interaction of longitudinally stiffened girders

D. Beg[1], F. Sinur[2]

Abstract
To understand the behavior of longitudinally stiffened plated girders subjected to high bending moments and shear forces, four tests on large scale test specimens were performed. The results of these tests were used to verify the numerical model, which was employed for further parametric studies. With a verified simplified numerical model a parametric nonlinear analysis was systematically carried out to determine the resistance of longitudinally stiffened plated girders. Based on 630 numerical simulations a new bending-shear interaction equation is proposed. An extensive reliability analysis of five different design models was made, i.e. the EN 1993-1-5 interaction model, the proposed new model, the gross cross-section bending resistance model and two models, which are combinations of the first three.

1. Introduction

In EN 1993-1-5 (CEN 2006) the interaction of bending moment and shear forces in plate girders takes into account the gradient of bending moment. Therefore the moment-shear interaction is checked at a distance of $h_w/2$ from the most stressed edge of the panel, where h_w denotes the web height. The interaction rule given in EN 1993-1-5 does not distinguish between longitudinally stiffened girders and longitudinally unstiffened girders. The interaction formula in EN 1993-1-5 was verified (Veljkovic, Johansson 2001) on unstiffened girders against experimental tests and numerical simulations. The tests and numerical simulations confirmed its validity. After EN 1993-1-5 was published, some doubts have been raised whether the same interaction formulation can also be used for longitudinally stiffened girders, especially because this formulation results in much higher resistance than interaction formulations in some national standards like (BS 5400-3, 2000) and (DIN 18800, 1990). To cover this gap experimental and numerical analysis of this topic was performed in the frame-work of the doctoral thesis (Sinur 2011).

2. Experimental program

The aim of four full scale tests, which were determined on the basis of previous numerical study (Sinur 2010), was to examine a characteristic behaviour of longitudinally stiffened plated girders under high bending and shear forces and to see, whether the current design rules given in EN

[1] Professor Darko Beg, University of Ljubljana, <darko.beg@fgg.uni-lj.si>
[2] Assistant Franc Sinur, University of Ljubljana, <franc.sinur@fgg.uni-lj.si >

1993-1-5 are adequate. Further on, the test results also served for the verification of numerical models.

The tests were performed on two girders stiffened with transverse and longitudinal stiffeners. On each of them two panels were investigated. One girder was made of symmetric cross-section and the other one of unsymmetrical cross-section. The transverse stiffeners were designed as rigid to prevent interaction between adjacent panels. The transverse stiffeners were designed taking into account deviation forces and tension field action in accordance with EN 1993-1-5 with analytical model given in (Johansson et al. 2007 and Beg and Dujc 2007). The relative flexural stiffness γ of longitudinal stiffeners was designed to prevent global buckling of the whole panel due to shear load. All four tests can be defined as follows:

- Symmetric Plated Girder with Open Stiffener (SO)
  $h_w / t_w = 214,\ \alpha = 1,0,\ \gamma = 41,55$
- Symmetric Plated Girder with Closed Stiffener (SC)
  $h_w / t_w = 214,\ \alpha = 1,5,\ \gamma = 95,76$
- Unsymmetrical Plated Girder with two Open Stiffeners (UO)
  $h_w / t_w = 300,\ \alpha = 1,0,\ \gamma = 52,12$
- Unsymmetrical Plated Girder with Closed Stiffener (UC)
  $h_w / t_w = 300,\ \alpha = 1,5,\ \gamma = 137,1$

2.1 Girder description and material

The length of the tested girders was 11.160 m and 11.325 m. In Fig. 1 and Fig. 2 the tested panels are noted as SO, SC, UO and UC. On a girder with symmetric cross-section plotted in Fig. 1 with the total height of 1544 mm panels SO and SC were tested. For both tested panels SC and SO the longitudinal stiffener was positioned in the compression zone of the web, 350 mm from the upper flange. The web in the part of the tested panels SO and SC (see Fig. 1) was 7 mm thick, which resulted in global slenderness of $h_w/t_w=214$. Double sided transverse flat stiffeners 156 × 20 mm were used at supports and at the load application point. With additional transverse stiffeners at both ends of the girder the rigid end post was assured.

Panels UO and UC were tested on the girder with unsymmetrical cross-section with the total height of 1840 mm as shown in Fig. 2. The web thickness of the tested panels was 6 mm. The unsymmetrical cross-section was chosen to have a larger compression area of the web, which resulted in higher compression force in the stiffeners. The positioning of the stiffeners at the compression part of the web can be seen in Fig. 2. The transverse stiffeners were designed in the same way as in the case of symmetric girder, which resulted in flat stiffener 122×20 mm. The geometry of each tested girder is summarized in Table 1.

Table 1: Geometry of the tested steel plate girders [mm]

	Web			Upper flange		Bottom flange		Longitudinal stiffener			
Specimen	h_w	t_w	a	b_{f1}	t_{f1}	b_{f2}	t_{f2}	H_{sl}	h_{sl}	b_{sl}	t_{sl}
SO	*1500*	*7*	*1500*	*320*	*22*	*320*	*22*	*/*	*/*	*90*	*10*
SC	*1500*	*7*	*2250*	*320*	*22*	*320*	*22*	*160*	*80*	*80*	*5*
UO	*1800*	*6*	*1800*	*250*	*20*	*450*	*20*	*/*	*/*	*100*	*10*
UC	*1800*	*6*	*2700*	*250*	*20*	*450*	*20*	*300*	*180*	*80*	*5*

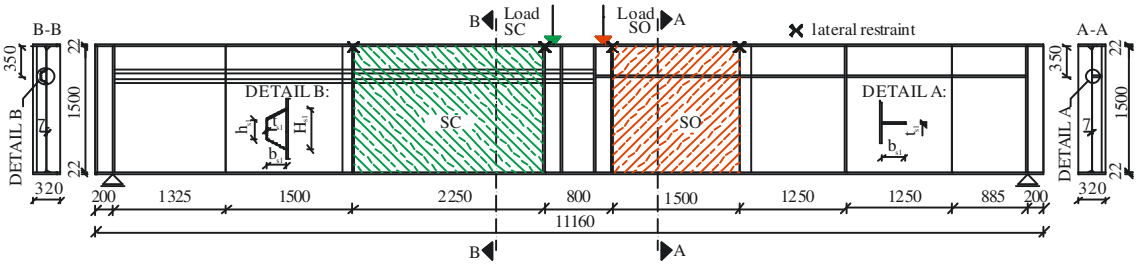

Figure 1: Girder geometry – Symmetric cross-section

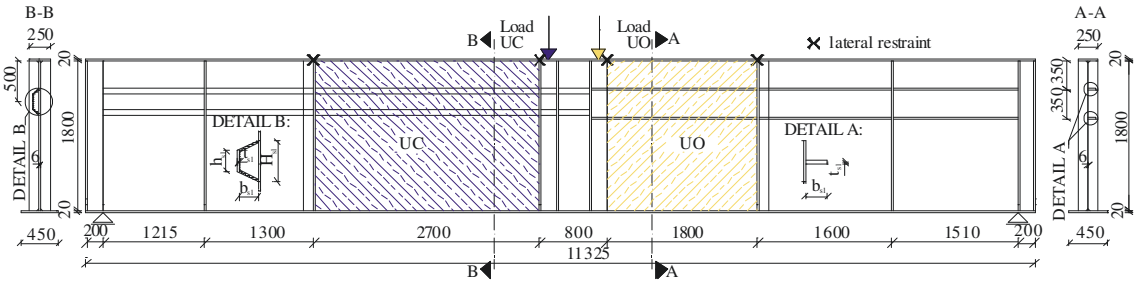

Figure 2: Girder geometry – Unsymmetrical cross-section

Table 2 summarizes the mechanical properties obtained from the tension tests for the web plate and flanges. The yield stresses and the ultimate stresses were defined as the average values of three tension tests per each plate. For each plate one static value was obtained and the average reduction of all measured yield values was calculated. The final static yield stress, which was considered in numerical simulations, was determined as a reduction of average yield stress.

Table 2: Results from tensile coupon-tests in plates

Plate	$R_{p\,02}$ Yield stress	R_m Ultimate stress	Average reduction of $R_{p\,02}$	Static yield stress
6 mm	*405 MPa*	*539 MPa*	*7,19 %*	*376 MPa*
7 mm	*391 MPa*	*561 MPa*		*363 MPa*
20 mm	*375 MPa*	*543 MPa*		*348 MPa*
22 mm	*354 MPa*	*536 MPa*		*328 MPa*

2.2 Test procedure

The tests were performed as three-point bending tests under static load (see Fig. 3). At both supports, the rotation around the axis perpendicular to the web plane and movement along the longitudinal axis were allowed. The load was applied by hydraulic actuator with maximum capacity of 3000 kN using a displacement control.

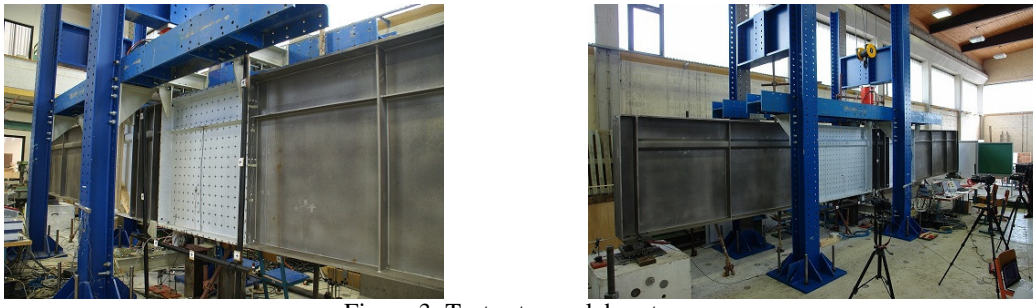

Figure 3: Test set-up – laboratory

After the test girder had been positioned in the testing frame, it was loaded up to approximately 15% of anticipated maximum load, which was still in elastic range.
After the preloading phase, the real test of the girder followed by applying static load in steps. The displacement velocity of the vertical displacement under hydraulic actuator was limited to 0,05 mm/s in elastic range and increased to 0.10 mm/s after the plastic response had been observed from the force-displacement curve. In selected load steps the loading was stopped to obtain static response of the girder's resistance.

2.3. Instrumentation

As the test progressed, strains, displacements and forces were continually measured. The strains in flanges, transverse stiffeners and longitudinal stiffeners were measured by using uni-axial strain gauges, whereas at some selected locations in the web rosette strain gauges were used. The deflections of the girder as well as out-of-plane displacements in some characteristic points were measured by using displacement transducers (LVDT) and digital dial indicators.
Photogrammetric method was used to determine displacement field of the tested panel at different loading levels. For this purpose the panel was painted white and marked with black crosses. Crosses were positioned to form a square net of 100×100 mm (see Fig. 4). At these points the displacements in all three directions were tracked at each step of the loading. Pilot measurements showed that the accuracy of the photogrammetric method was below 0.2 mm.

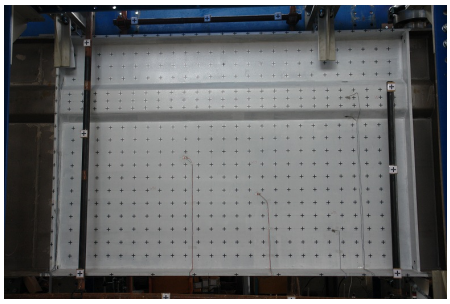

a) Panel marked with black crosses

b) Position of the two digital cameras

Figure 4: Setup of tested panels for photogrammetry

2.4. Initial imperfections

The initial imperfections have to be properly considered in numerical model verification. The most important initial imperfections present in plated girders are geometrical imperfections w_0 and residual stresses σ_R. The initial geometric imperfections were measured in all four tested panels, while residual stresses were measured only in one cross-section.

2.4.1 Geometrical imperfections

The initial geometry of the tested web panels was precisely determined by employing photogrammetric method. In all other regions the geometry and imperfections were measured using laser distance measuring device. The 3D data format determined by digital linear transformation was interpolated on a grid of 10×10 mm using MATLAB 4 griddata method.
Fig. 5a represents initial imperfections measured on tested panel SO. The maximum imperfection is observed in the largest subpanel with the amplitude of – 5.75 mm. The web plate is much less imperfect near longitudinal stiffener. Along the stiffener the maximum deviation of 0.92 mm is obtained.

The measured imperfections of panel SC are plotted in Fig. 5b. The shape of initial geometry is similar to panel SO with maximum amplitude of -5.79 mm observed in the largest subpanel. The maximum amplitude of the smallest subpanel was 1.85 mm and was obtained at the left side of the plate.

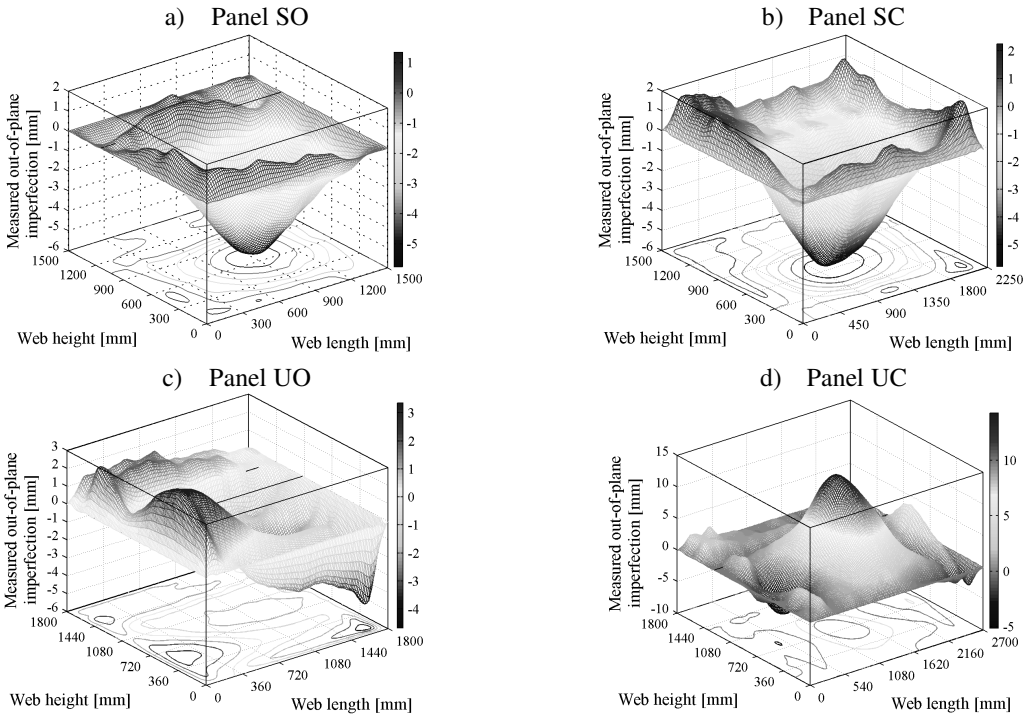

Figure 5: Measured initial imperfections in the tested panels

Fig. 5c represents the imperfections of UO web panel stiffened with two open stiffeners. In this situation the imperfection shape is rather unusual, as the maximum amplitudes were measured in the vicinity of transverse stiffeners. In horizontal direction an S-shape initial imperfection was observed with maximum and minimum amplitude of 3.36 mm and 4.67 mm, respectively. The imperfections of both stiffeners were of C-shape; stiffener at x = 1450 mm had imperfection with the maximum amplitude of 2.29 mm and stiffener at x = 1100 mm -2.02 mm. The overall maximum imperfection amplitude 2.51 mm of the subpanel was found in the left corner of the web.

Initial imperfections of the web panel UC (see Fig. 5d) do not originate only from cutting and welding during the production process itself, but also from previous testing of the UO panel. The reason for this is the fact that after unloading of the first test the girder did not return completely in to the initial state. The maximum initial imperfection of 14.27 mm was obtained in the largest subpanel and -3.08 mm in the minor subpanel. The stiffener remained straight during the loading of neighboring panel in the previous test and the measured initial imperfections were 2.49 mm. In comparison to allowable tolerances according to EN 1090-2 (CEN 2008) only the initial imperfection in the panel UC was slightly higher than the allowable tolerance (11.5 mm).

2.4.2 Residual stresses

The magnitude and distribution of residual stresses in plated girders are primarily governed by the welding and cutting of the plates.

To find out the real distribution of normal residual stresses in longitudinal direction, sectioning method was applied to the part of unsymmetrical girder UC, which was not exposed to high bending moments and shear forces during the test. After the test had been done, the residual stress measurement was performed using destructive sectioning method. The strain gauges were placed on both sides of the web and of the top flange using uni-axial strain gauges oriented in the longitudinal direction of the girder. Position of strain gauges is identified in Fig. 6.

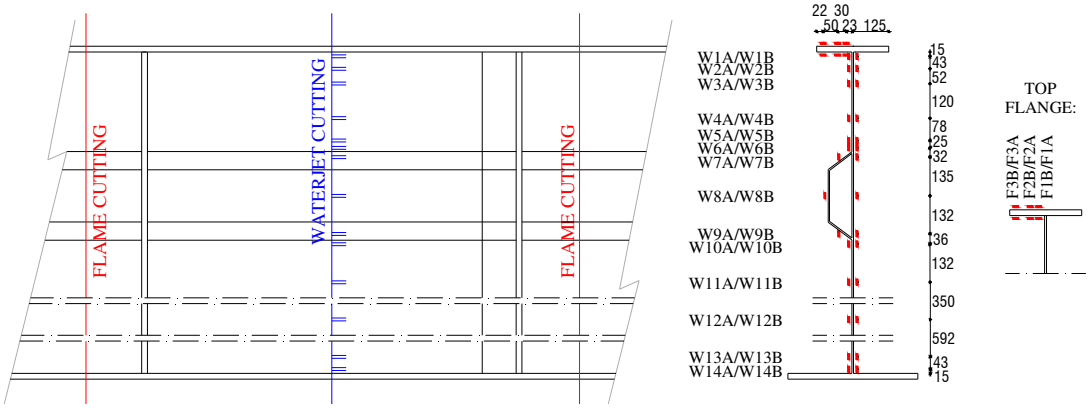

Figure 6: Positions of measured residual strains

The residual stress distributions in the web plate and in the investigated half of the flange are shown in Fig. 7. The stress distribution over the web depth is expected as large tension stresses in the vicinity of the welding and low compression stresses in other areas. The maximum tension stress in the web was measured 15 mm from the bottom flange and the average of both side measurements was 246 MPa. The average compression stress in the smallest subpanel was 40,60 MPa. In the largest subpanel on each side of the plate only 5 strain gauges were installed. Three of them were placed close to where the tension stresses were expected and two of them were out of this region, i.e. in the area where compression was expected. The average compression stress in this subpanel results in 7.89 MPa.

The residual stresses in plated girders are rather low compared to the residual stresses in other types of steel structural elements. The main parameter which influences residual stresses is of course the ratio between the input energy and the mass of the built-in material, which is in the case of plated girders low.

In case of thin web plates some of residual stresses are transformed to the initial deformations of the plate. Therefore, actual residual stresses are much lower than would be obtained for a compact plate.

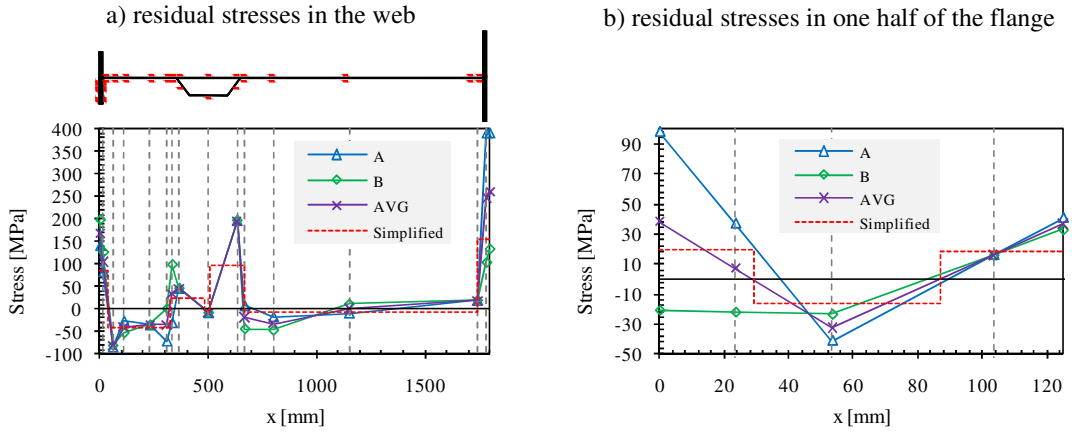

Figure 7: Measured residual stresses

2.5 Results

In Fig. 8 load-displacement curves for the tested girders are plotted. The force applied on the girder through hydraulic actuator is presented on the ordinate axis, while the deflection of the girder under the applied load is displayed on the abscissa axis. The testing procedure is the reason for the drops in girder resistance obtained in plastic zone, as the strain speed was set to 0. Because the loading speed is eliminated at these points, the lower bound of these drops represents the static response of the girder.

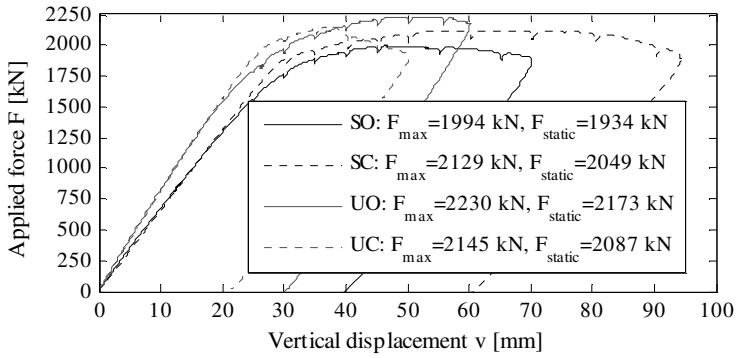

Figure 8: Load – Displacement curves for tested girders

Since more than one parameter was varied at tests, the comparison between the girder resistances is not very consistent. However, the highest resistance was proven at unsymmetrical girder stiffened with two open stiffeners and the smallest resistance was obtained for symmetric girder stiffened with one open stiffener. All girders show a linear elastic response up to a high load level and as they pass over to the plastic range, the load gradually increases up to the maximum resistance. Once the maximum capacity is reached, the load gradually decreases. For both symmetric girders and the UO girder the decrease of their resistance after reaching the peak force is moderate, which results in high rotational capacity. At the UC test lower ductility is obtained due to local instability of the longitudinal stiffener.

2.5.1 Web buckling of tested panels

The evolution of the out-of-plane displacements of the tested panels is plotted in Fig. 9. The displacement fields are plotted for the following characteristic points: in elastic zone at vertical displacement of 20 mm, in plastic zone at vertical displacement of 35 mm and the last one at the maximum load obtained in each test.

At load stage v = 20 mm, where the load of the panel is already higher than elastic critical shear force of the largest subpanel, typical shear buckling in the largest subpanel is observed. By increasing the shear force in the girder, the bending moment increases, which causes buckling in the smaller sub-panel subjected to high compression stress. The buckling shape depends on the level of shear and bending stresses. When the girder resistance is exhausted, combination of shear buckling and flexural buckling is observed, except for the UO panel where a clear separation of failure modes developed because the lower longitudinal stiffener was out of the danger zone with high compression stresses.

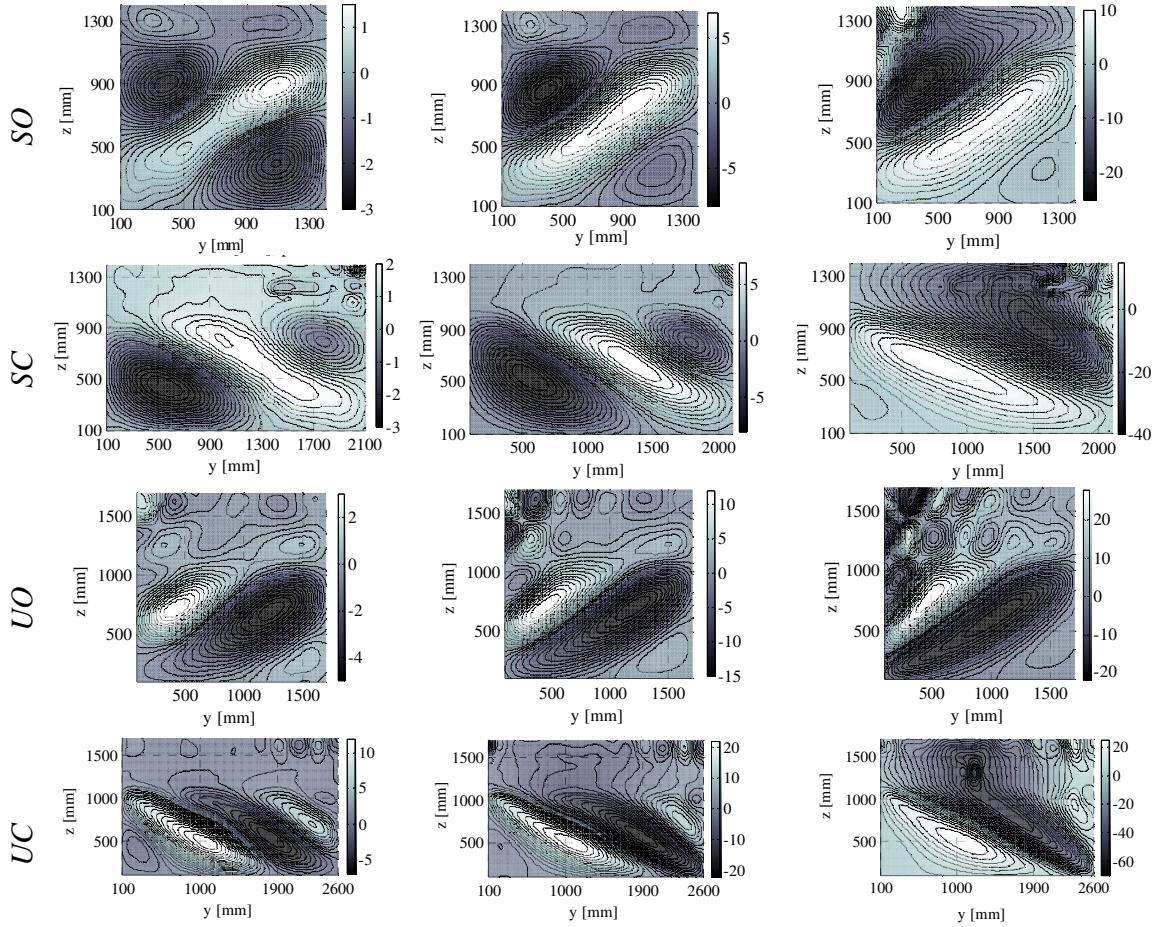

v = 20 mm v = 35 mm v = v(F_{max})

Figure 9: The development of out of plane displacement

3. Numerical verification

The numerical model was developed in the general-purpose code ABAQUS. In numerical model the measured initial geometrical imperfections and nonlinear material behaviour based on tensile tests were considered. The material was modeled with static values.

The verification of numerical model was performed by comparing initial stiffness, maximum capacity and failure modes.

The load-deflection curves of the tested girders and numerical simulations are plotted in Fig. 10. The response of numerical simulations fits experimental results well.

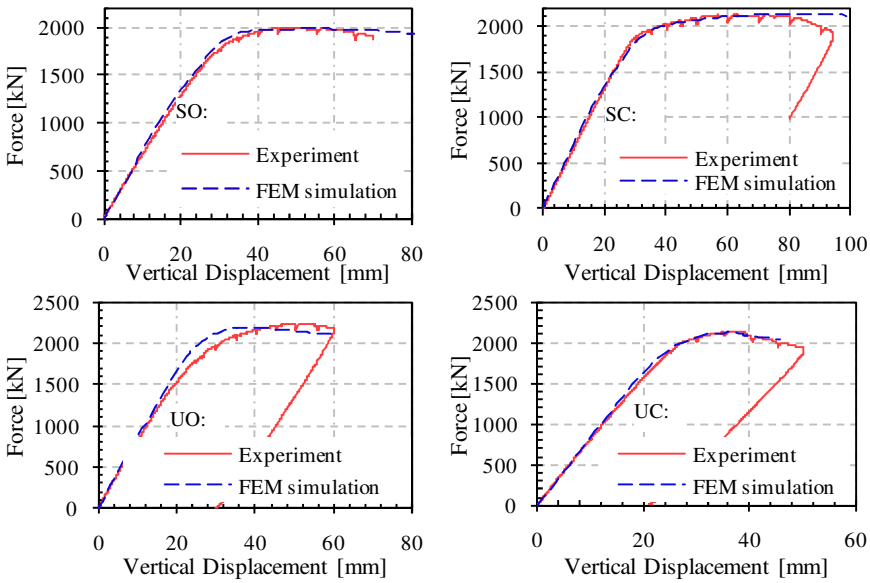

Figure 10: Load-deflection curves: Comparison of experimental and numerical results

The evolution of the out-of-plane displacement of the web panel obtained by numerical simulation and experimentally measured results are plotted in Fig. 11. Comparing these results, the following conclusions can be given:

- In general the out-of-plane displacement is similar to the experimentally measured shape.
- In plastic range the absolute maximum amplitude calculated with numerical simulations approaches the measured experimental value.
- The local buckling of the flange in compression developed in the opposite direction compared to the direction found in experimental test.

The numerical model sufficiency describes the behavior of the real test. With proper consideration of significant parameters, such as real material model, proper mesh density and actual initial imperfections, the numerical results can get very close to the real behavior of experimental test, as in presented situation.

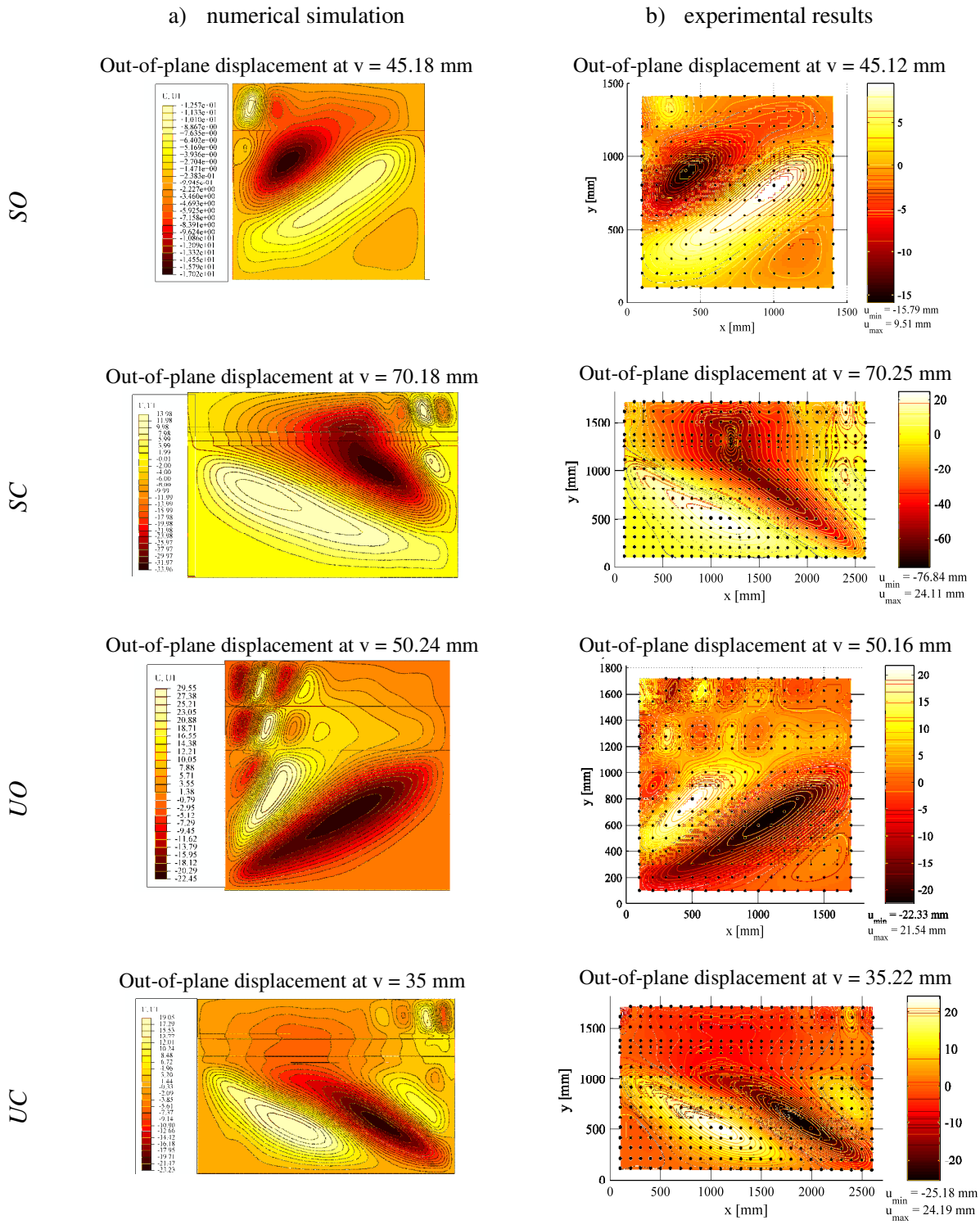

Figure 11: The evolution of the out-of-plane displacement

The results of experimental tests and numerical simulations are gathered in Table 3. The maximum difference of 4,1% in girder resistance is found for girder SC. In all cases the resistance obtained by numerical simulations is slightly higher than experimentally obtained.

Table 3: Comparing experimental resistance with resistance according to EN 1993-1-5

	TPS 1	TPS 2	TPS 3	TPS 4
$F_{Eksperiment}$ [kN]	*1934*	*2049*	*2173*	*2087*
F_{ABAQUS} [kN]	*1991*	*2134*	*2186*	*2125*

4. Parametric study

To analyse post-critical resistance of girders under high bending and shear load, a parametric study was performed using ABAQUS code. The simulations were performed on a girder with four panels (see Fig. 12). The girder was vertically supported in the girder half-length were double side stiffeners were applied. On each side of the girder the combination of shear load and bending moment was applied.

The following parameters were considered to investigate M-V interaction of longitudinally stiffened plated girders:

- GROUP I: Flange to web cross-section ratio (A_f/A_w),
- GROUP II: Web slenderness (h_w/t_w),
- GROUP III: Panel aspect ratio ($\alpha=h_w/t_w$),
- GROUP IV: Stiffness of longitudinal stiffeners.

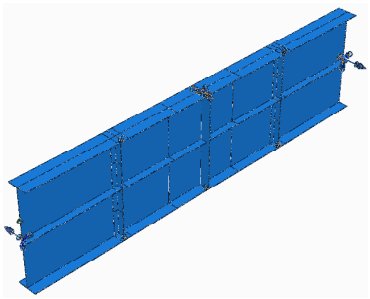

Figure 12: Numerical model

The numerical database was constructed by varying the aforementioned parameters. Four groups formed the framework of the sample. Each group consisted of a web panel height of h_w = *2000 mm* and within each group the panel was subjected to 5 different bending moment – shear force ratios. Four ratios were selected to be in the interaction zone according to EN 1993-1-5. The last ratio was selected at shear load equal to 60% of pure shear capacity of the web V_{bw}. Within each group the following parameters are additionally varied: shape of longitudinal stiffeners (open I stiffener, closed stiffener), position and number of longitudinal stiffeners (n = *1, 2*). The vertical position of longitudinal stiffeners was varied only for one stiffener ($h_w/4$, $h_w/2$); in the first case the web was stiffened in the compression part, so the stiffener was subjected to high compression force, and in the second case the stiffener was positioned at half web depth. When two stiffeners were applied, they were positioned equidistantly. For the girder stiffened with two longitudinal stiffeners the range of parameters was reduced. The material was modeled as elastic-plastic with a small hardening. The yield stress and elastic modules were taken as nominal values.

4.1 Evaluation of M-V interaction acc. to EN 1993-1-5

The characteristic resistance was calculated and compared to the results of numerical simulations. The internal forces obtained with numerical model were evaluated at a distance $min(a, h_w/2)$ and $h_{wi,max}/2$ from the most stressed edge, where a is the length of the panel and $h_{wi,max}$ is the maximum height of the subpanels.

The numerical results are plotted on the M-V interaction domain. The results which are below the interaction curve in the range of M_f to $M_{el,eff}$ are on the unsafe side and, vice versa, if the results are above the interaction curve, they are safe.

The numerical results for group I are plotted in Fig. 13. They are plotted in the non-dimensional format. The shear load is normalized with the characteristic shear resistance of the web and the bending moment with the characteristic plastic bending resistance. For each A_f/A_w ratio a different M-V interaction curve should be plotted, but in the figure only two interaction curves for ratios of $A_f/A_w = 0.3$ and $A_f/A_w = 1.1$ are shown. Vertical lines which denote the effective characteristic resistance of the girder for the same ratios are added. The numerical results are plotted for girders stiffened with open and closed stiffeners positioned at $h_w/4$ and $h_w/2$.

All girders that were stiffened with one stiffener at $h_w/4$ show higher resistance than the one predicted in accordance with EN 1993-1-5. When the stiffener is positioned in the mid web depth and the interaction is checked at a distance of $min(a, h_w/2)$, the numerical resistance is found on the unsafe side if in the middle part of M-V interaction. When the interaction is checked at a distance of $h_{wi,max}/2$, the numerical resistance is always on safe side. Linear interaction between bending moment and shear force was found for all studied cases.

The numerical results for group II, where the varied parameter is the slenderness of the web, are plotted in Fig. 14. The difference between M-V interaction curves for various slendernesses is negligible, therefore only one interaction curve was plotted. The only difference obtained for different slendernesses of the web is the vertical line which denotes elastic effective bending resistance. The first and the second vertical line belong to girders with the highest slenderness, stiffened with stiffener at the mid web depth (first line) and at $h_w/4$ (second line). The other two vertical lines, which are virtually the same, belong to girders with the lowest slenderness.

The results are plotted for girders stiffened only with one longitudinal stiffener. For interaction check at a distance of $min(a, h_w/2)$, the numerical resistance is higher for all girders stiffened with longitudinal stiffener in compressed part of the web ($h_w/4$) and for girders stiffened at mid web depth with web slenderness $h_w/t_w > 200$. For interaction check at $h_{wi,max}/2$ all numerical results, except girder with low slenderness $h_w/t_w = 150$ and stiffener at mid web depth, prove higher resistance. The influence of tension stresses in the largest subpanel results in higher shear resistance, which can clearly be seen from Fig. 14.

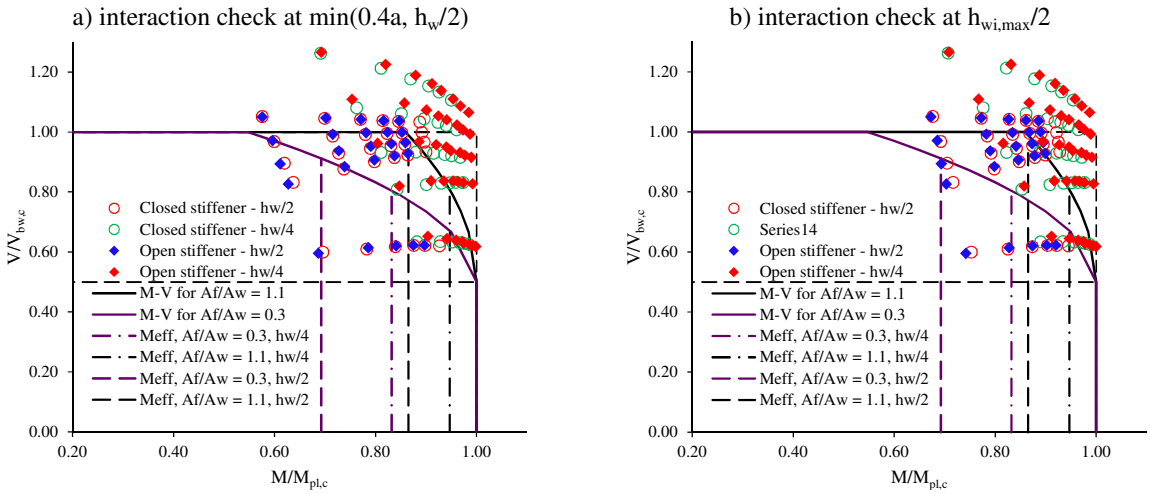

Figure 13: Numerical results plotted on current formulation of M-V interaction - GROUP I

The shape of the interaction curve depends on the slenderness of the web. For higher slendernesses $h_w/t_w \leq 200$ the shape of interaction is linear, while for slenderness $h_w/t_w = 150$ a nonlinear interaction is observed.

The numerical results of group III, where the influence of a panel aspect ratio was studied, and the results of group IV, where the influence of stiffness of longitudinal stiffener was investigated, are plotted in Fig. 15 and Fig. 16, respectively. In both cases only one interaction curve corresponds to all calculations. The difference is only in vertical lines which indicate elastic effective bending resistance of the studied girders. The results are plotted only for girders stiffened with one stiffener.

The same conclusions can be drawn for these two groups. Girders, where the sub-panel critical in shear is under tension, show much higher resistance. On the other hand when this sub-panel is under compression (this is found for girders stiffened with one stiffener in mid-panel and for girders stiffened with two equidistantly spaced stiffeners), the girder resistance is smaller than the one obtained with EN 1993-1-5 for interaction check at *min(a, h_w/2)*.

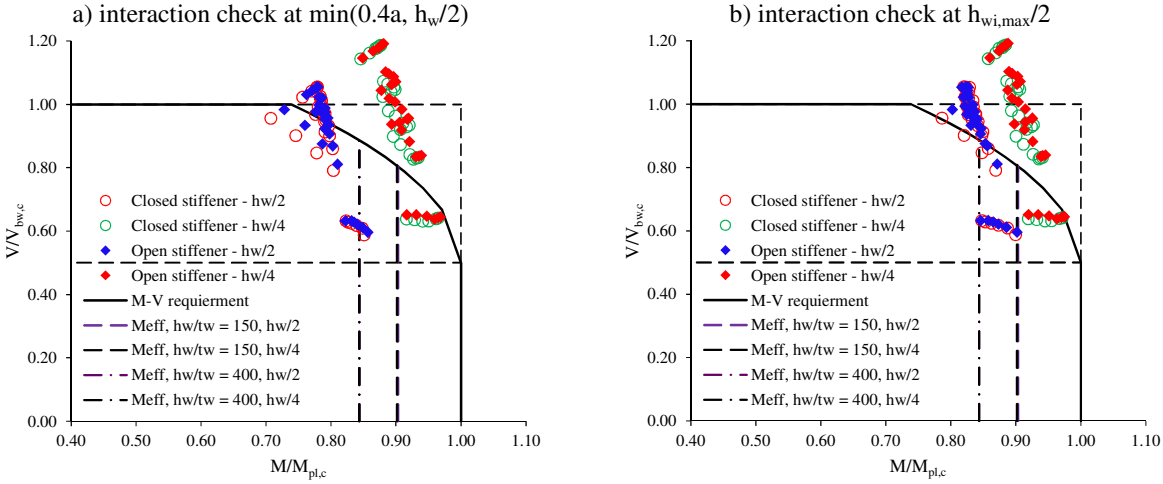

Figure 14: Numerical results plotted on current formulation of M-V interaction - GROUP II

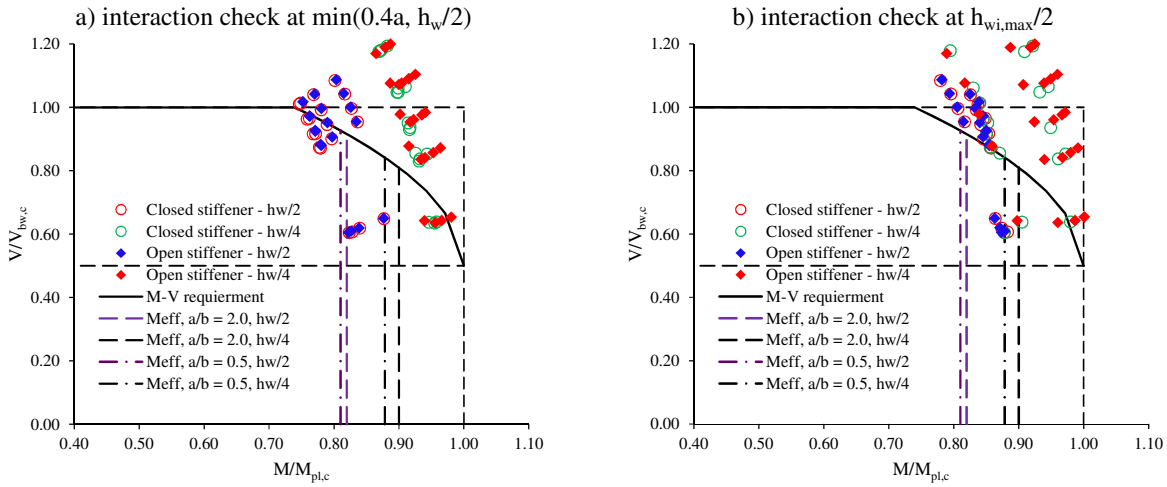

Figure 15: Numerical results plotted on current formulation of M-V interaction - GROUP III

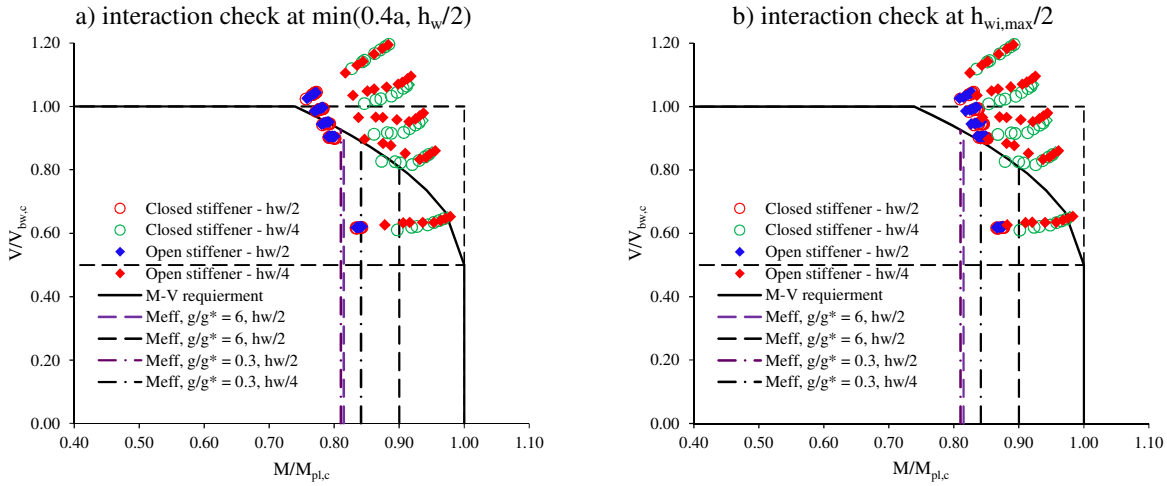

Figure 16: Numerical results plotted on current formulation of M-V interaction - GROUP IV

4.2 New proposal for M-V interaction

The evaluated results show that the existing interaction formula which was evaluated at a distance of *min(a, h_w/2)* and at *$h_{wi,max}$/2* from the most stressed edge does not always accurately describe actual behaviour. First, the current interaction curve is described with a quadratic formula while the obtained response of numerical results is in most cases linear. Secondly, the interaction formula at distance of *min(a, h_w/2)* gives safe results only for girders that possess longitudinal stiffener at a distance of *h_w/4*. Therefore, for the area of large bending moment and shear force a new interaction equation is proposed and defined as:

$$\bar{\eta}_{1,new} + \left(1 - \frac{M_{f,Rd}}{M_{el,eff,Rd}}\right)\left(2\bar{\eta}_3 - 1\right)^{\kappa} \le 1,0 \qquad (1)$$

with

$$\overline{\eta}_{1,new} = \frac{M_{Ed}}{M_{el,eff,Rd}}$$

.

The differences compared to previous interaction formula are: plastic bending resistance $M_{pl,Rd}$ is replaced with elastic effective bending resistance $M_{el,eff,Rd}$, power κ is in the first approximation taken as $\kappa = 1$. Both interaction relations valid for bending moment $M_{f,Rd} \leq M_{Ed} \leq M_{el,eff,Rd}$ are plotted in Fig. 17. The new formula gives the same resistance as the current one, when bending moment is equal to bending capacity of flanges. For all other load combinations, the new proposal results in lower resistance.

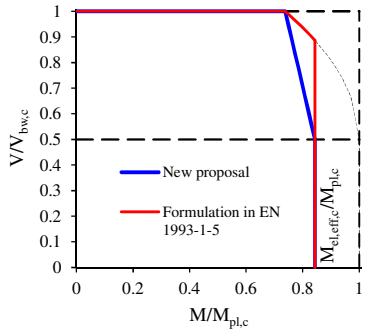

Figure 17: M-V interaction formulation – comparison

4.3 Determination of partial safety factor

In engineering practice the resistance of the structure is defined with design values where uncertainties of the material, geometry and the model are considered. In this chapter the interaction resistance model is statistically evaluated. Mean values, standard deviations and coefficient of variations are calculated. The model is developed on the basis of numerical simulations, therefore the coefficient of variation which takes into account numerical model is also considered. Partial safety factors were determined according to EN 1990 Annex D (CEN 2004).

4.3.1 Resistance models

Five resistance models were evaluated to determine partial safety factors: two interaction models, one gross cross-section resistance model and two combined models. To take advantage of the moment gradient the interaction models were evaluated at sections 1-1 and 2-2 as shown in Fig. 18, while the check to gross cross-section bending resistance is performed at section 0-0. The first resistance model $r_{t,1}$ corresponds to the interaction check according to EN 1993-1-5. Since the interaction formulation does not fit the shape of interaction, a new resistance model was introduced (Chapter 4.2) and is denoted as resistance model $r_{t,2}$. When the moment gradient is accounted for, EN 1993-1-5 requires an additional check of bending resistance of gross cross-section at the most stressed edge of the panel (section 0-0). Therefore, the third resistance $r_{t,3}$ model which represents bending check of the gross cross-section was evaluated.

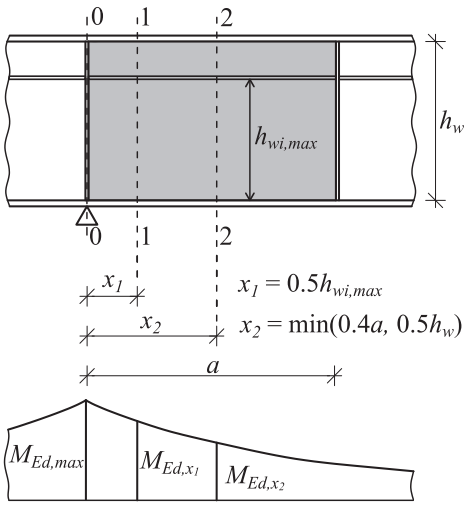

Figure 18: Position of interaction check (sections 1-1 and 2-2) and gross cross-section check (section 0-0)

The first theoretical model is the existing M-V interaction formula given with the following expression:

$$r_{t,1} = V = \left(1 + \left(\frac{M_{pl,c} - M}{M_{pl,c} - M_{f,c}} \right)^{0.5} \right) \cdot \frac{V_{bw,c}}{2}. \tag{2}$$

The second numerical model is a new proposed M-V interaction formula determined with equation:

$$r_{t,2} = V = \left(1 + \left(\frac{M_{el,eff,c} - M}{M_{el,eff,c} - M_{f,c}} \right) \right) \cdot \frac{V_{bw,c}}{2}. \tag{3}$$

The third resistance model is defined as elastic bending resistance of a gross cross-section checked at the edge of the panel:

$$r_{t,3} = V = \frac{M_{el,c}}{l}. \tag{4}$$

The models were evaluated for the following sub-sets:

- Sub-set I: All analysed girders - 582 data,
- Sub-set II: Only girders stiffened with longitudinal stiffener at $h_w/4$,
- Sub-set III: Only girders stiffened with longitudinal stiffener at $h_w/2$,
- Sub-set IV: Only girders stiffened with two equally spaced longitudinal stiffeners.

4.3.2 Comparison and evaluation of results

The results of evaluated partial safety factors are gathered in Table 4 to Table 6. The partial factors were determined for three theoretical models on four sub-sets. The largest partial factor is found for interaction model $r_{t,1}$ on sub-set IV, where the results of girders stiffened with two

longitudinal stiffeners are treated. The new proposed interaction formula results in smaller partial factors for all sub-sets.

When the interaction resistance model is checked at a distance of *min(0.4a, h_w/2)*, the partial safety factor is smaller than partial safety factor γ_{M1} =1.1 given in EN 1993-1-5 only for sub-set II for both models (1.048 and 0.999, see Table 4) and for sub-set III for resistance model $r_{t,2}$ (1.096, see Table 4). In all other cases the partial safety factor is above γ_{M1} =1.1, especially for sub-set IV. The lowest partial safety factor is found for girders stiffened with one stiffener in compression zone. This is because the resistance model does not consider the increase of shear resistance due to tension stresses in the lower sub-panel.

The partial factors evaluated for the interaction check at a distance of $h_{wi,max}$/2 from the most stressed edge are gathered in Table 5. For this interaction check location the partial safety factors are logically smaller. If all numerical results are evaluated, the partial safety factor for resistance model $r_{t,1}$ is 1.103 and for model $r_{t,2}$ 1.033 (see Table 5, sub-set I). The largest factor is obtained for sub-set IV where γ_M = 1.113 for resistance model $r_{t,1}$ and γ_M = 1.051 for resistance model $r_{t,2}$. The difference between partial safety factors evaluated for all sub-sets is for the interaction check at $h_{wi,max}$/2 much smaller than for the check at a distance of *min(a, h_w/2)*.

Table 4: Calculated γ_M values for resistance models $r_{t,1}$ and $r_{t,2}$ at min(0.4a, h_w/2)

Sub-set	*b*		V_δ		V_r		γ_M	
	$r_{t,1}$	$r_{t,2}$	$r_{t,1}$	$r_{t,2}$	$r_{t,1}$	$r_{t,2}$	$r_{t,1}$	$r_{t,2}$
I	*1.0050*	*1.0430*	*0.060*	*0.056*	*0.106*	*0.104*	***1.157***	***1.111***
II	*1.0997*	*1.1445*	*0.049*	*0.036*	*0.101*	*0.095*	***1.048***	***0.999***
III	*0.9993*	*1.0340*	*0.031*	*0.017*	*0.093*	*0.089*	***1.140***	***1.096***
IV	*0.9432*	*0.9803*	*0.048*	*0.040*	*0.100*	*0.096*	***1.221***	***1.168***

Table 5: Calculated γ_M values for resistance models $r_{t,1}$ and $r_{t,2}$ at $h_{wi,max}$/2

Sub-set	*b*		V_δ		V_r		γ_M	
	$r_{t,1}$	$r_{t,2}$	$r_{t,1}$	$r_{t,2}$	$r_{t,1}$	$r_{t,2}$	$r_{t,1}$	$r_{t,2}$
I	*1.0491*	*1.1067*	*0.055*	*0.037*	*0.103*	*0.095*	***1.103***	***1.033***
II	*1.1033*	*1.1485*	*0.050*	*0.040*	*0.101*	*0.096*	***1.045***	***0.998***
III	*1.0408*	*1.0925*	*0.019*	*0.016*	*0.090*	*0.089*	***1.089***	***1.037***
IV	*1.0264*	*1.0881*	*0.036*	*0.037*	*0.095*	*0.095*	***1.113***	***1.051***

Table 6: Calculated γ_M values for resistance model $r_{t,3}$

Sub-set	*B*	V_δ	V_r	γ_M
I	*1.0493*	*0.054*	*0.103*	***1.103***
II	*1.1240*	*0.035*	*0.094*	***1.016***
III	*1.0184*	*0.017*	*0.089*	***1.113***
IV	*1.0280*	*0.029*	*0.092*	***1.107***

The partial safety factors evaluated for resistance model $r_{t,3}$ are gathered in Table 6. The partial safety factor for gross cross-section check in EN 1993-1-5 is equal to γ_{M0} =1.0. For all sub-sets the determined partial safety factors for model $r_{t,3}$ were found higher than the one given in EN 1993-1-5. The maximum factor γ_M = 1.113 is found for sub-set III. This result is very important from the simplification point of view, because the interaction check can be completely replaced with the much simpler gross cross-section check at the edge of the panel with the maximum value of a bending moment.

5. Conclusions

The following conclusions can be drawn on the basis of experimental and numerical analysis of longitudinally stiffened girders subjected to the combination of high bending moment and shear load:

- All four tested girders exhibit much higher resistance than was obtained by EN 1993-1-5. The reason for this is stabilizing effect of tension stresses in the largest subpanel which is not considered in the resistance model,
- Through load-deflection curve large ductility was obtained for three girders, while girder UC showed smaller ductility due to buckling of the longitudinal stiffener which was in class 4 cross-section,
- Typically the failure mode was characterized by combination of shear buckling of the web plate and flexural buckling of the longitudinal stiffener,
- An extensive parametric study showed that the interaction formula depends on the slenderness of the web, and the M-V relation is found linear for most cases. Therefore a new interaction formula is proposed,
- The reliability analysis of three different resistance models showed that the reliability conditions are met for all three models if the interaction check is performed at a distance of $h_{wi,max}/2$ (models $r_{t,1}$ and $r_{t,2}$) and if the partial safety factor $\gamma_M = 1.1$ is introduced when calculating shear resistance of the girder,
- The resistance model $r_{t,3}$ – elastic gross cross-section resistance can completely replace the existing M-V interaction check in EN 1993-1-5 if the partial safety factor γ_M is taken equal to 1.1 and the check is performed for the maximum moment of the panel.

References

CEN (2006). EN 1993-1-5: Design of steel structures - Part 1-5: Plated structural elements, Brussels, European Committee for Standardisation

Veljkovic, M. and Johansson, B. (2001). Design for buckling of plates due to direct stress. Proceedings of the Nordic Steel Construction Conference Helsinki

BS 5400-3.(2000). Steel, concrete and composite bridges - Part 3: Code of practice for design of steel bridges

DIN 18 800 Teil 3. (1990). Stahlbauten - Stabilitätsfälle, Plattenbeulen. Berlin, Beuth verlag GnbH

Sinur, F. (2011). Behaviour of longitudinally stiffened girders under combination of high bending and shear load. Doctoral Thesis, Faculty of civil and geodetic engineering, University of Ljubljana, Ljubljana, 205 p.

Sinur, F. and Beg, D. (2010). Behaviour of longitudinally stiffened plate girders subjected to bending and shear. Proceedings of the Annual Stability Conference, Missouri University of Science and Technology, Orlando, Florida

Johansson, B., et al. (2007). Commentary and worked examples to EN 1993-1-5 "Plated Structural Elements", in JRC Scientific and Technical Reports

Beg, D. and Dujc, J. (2007). On stability of transverse stiffeners. Proceedings of the Annual Stability Conference, University of Missouri-Rolla, New Orleans, Louisiana

CEN (2004). EN 1990: Eurocode-Basis of structural design. Brussels, European Committee for Standardisation

CEN (2008). EN 1090-2: Execution of steel structures and aluminium structures – Part 2: Technical requirements for steel structures. Brussels, European Committee for Standardisation